MULTIDENTATE LIGAND EXCHANGE KINETICS: REACTIONS OF AMINOCARBOXYLATO– FERRATE(III) COMPLEXES WITH 4–(2–PYRIDYLAZO) RESORCINOL

NISHI GUPTA and PREM C. NIGAM*

(*Department of Chemistry, Indian Institute of
Technology, Kanpur–208 016, India*)

The kinetics and mechanism of ligand substitution reactions of nitrilotriacetatoiron(III), [Fe(NTA)], and N–(2–hydroxyethyl)–ethylenediaminetriacetatoiron(III), [Fe(HEDTA)], complexes with 4–(2–pyridylazo) resorcinol (Par) has been investigated at $pH = 9.0 \pm 0.02$, $I = 0.1 \, mol \cdot l^{-1}$ (NaClO$_4$), and temp. $= 25 \pm 0.1 ℃$ and $30 \pm 0.1 ℃$ respectively. The reaction has been studied spectrophotometrically at 496 nm. (λ_{max} of Fe(Par)$_2$). In both reactions the final product was [Fe(Par)$_2$]$^-$. The values of second order rate constants for NTA and HEDTA exchange reactions are $(10.0 \pm 0.8) \times 10^1 \, l \cdot mol^{-1} \cdot s^{-1}$ and $(2.7 \pm 0.1) \times 10^{-1} \, l \cdot mol^{-1} \cdot s^{-1}$ respectively. The reactions of NTA and HEDTA exchange were studied in the pH range 6–9.5 and 7–10.85 respectively. The rate of reacton of [Fe(NTA)] with HPar$^-$ first increases with pH and then levels off. However, in the case of [Fe(HEDTA)] reaction, the rate increases monotonically with increase of pH in the specified range.

The reverse reactions between [Fe(Par)$_2$]$^-$ and L^{3-} (L = HEDTA or NTA) have been studied in the presence of large excess of L^{3-}.

The reaction is pseudo–first–order and zero order in ligand at high and low ligand concentrations respectively and inverse first order in Par concentration. Activation parameters for forward and reverse reactions have been calculated and used to support the proposed mechanism.

Keywords: kinetic multidentate exchange aminocarboxylatoferrate(III) Par

Introduction

Ligand substitution reactions of metal complexes with multidentate ligands have been studied by many authors.[1–10] A ligand substitution reaction often proceeds through a mixed–ligand complex intermediate, in which the central metal ion is simultaneously bonded to both leaving and entering ligands. In general, the rate determining step of the reaction is the

---

cleavage of one of the bonds between metal ion and the leaving group. For instance, [Ni(EDDA)] and [Ni(NTA)]⁻ react with Par to give mixed—ligand complex intermediates viz. [Ni(EDDA)Par]²⁻ and [Ni(NTA)Par]³⁻, respectively[9] (EDDA²⁻ = Ethylenediamine N,N′—diacetate ion, NTA³⁻ = Nitrilotriacetate ion) followed by further reaction to give Ni(Par)₂. Tanaka et al.[11] have studied the substitution reactions of [Cu(EGTA)]²⁻ and [Cu(NTA)]⁻ with Par [EGTA = (Ethylene glycol) bis (2—aminoethyl ether)—N,N,N′,N′—tetraacetate]. Similar results were noticed also in these reactions.

It seemed worthwhile to extend the study to the substitution reactions involving other metal ions, e.g. the ligand substitution reaction of [Fe(NTA)] and [Fe(HEDTA)] complexes with Par in alkaline medium represented by equation (1).

$$[FeL(OH)]^- + 2HPar^- \rightleftharpoons [Fe(Par)_2]^- + L^{3-} + H_2O + H^+ \qquad \cdots(1)$$
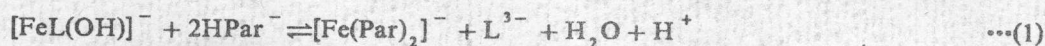
(L = NTA or HEDTA)

The investigation was undertaken to obtain a better understanding and insight into multidentate exchange processes. The kinetics of reverse reactions have also been investigated to provide support for the proposed mechanism.

Experimental

Chemicals

Purified and recrystallized varieties of NTA (Hopkin and Williams, England), HEDTA (Sigma, U.S.A), Par (Reidel, Germany), ferric nitrate (Thomas and Baker, U.K.) and sodium perchlorate (E. Merck, F.R.G.) were used in this study. Sodium tetraborate and sodium hydroxide were used to prepare buffers of desired pH values.

A stock solution of $Fe(ClO_4)_3$ was prepared by dissolution of a precipitate of $Fe(OH)_3$ in calculated amount of $HClO_4$ and standardized complexometrically using sulfosalicylic acid as an indicator.[12]

Equipment

A Shimadzu double beam spectrophotometer model UV—240, with a circulatory arrangement for thermostating the cell compartment was used for all kinetic studies and for obtaining repetitive scans of the reaction mixtures. The temperature of the reaction mixtures was maintained by an ultracryostat model 2 NBE (VEB Kombinat Medizin and Labortechnik Kombinatsbetrieb, GDR). All pH measurements were made on an Elico digital pH meter model LI—120 using BDH standard buffers for standardization.

Kinetic Measurements

The rate of formation of $[Fe(Par)_2]^-$ was measured at 496nm (λ_{max} of $[Fe(Par)_2]^-$, $\varepsilon = 51,800 \ 1 \cdot mol^{-1} \cdot cm^{-1}$) at pH = 9.0 ± 0.02 and I = 0.1mol $\cdot 1^{-1}$ (NaClO₄). A correction was applied for the absorbance of Par at 496 nm. It can be derived that

$$C_A = (A_t - \varepsilon_B C_B^o) / (\varepsilon_A - 2\varepsilon_B)$$

where C_A represents the concentration of $[Fe(Par)_2]^-$ at $t = t$ and C_B° is the concentration of Par at $t = 0$, while ε_A and the molar extinction coefficients of A and B in order. In the following text the aminocarboxylato complexes will be represented by [FeL] for the sake of simplicity while Par will be abbreviated as R.

The reverse reactions were also studide at 496 nm by the decay of $[Fe(Par)_2]^-$. An expression, with the absorption correction applide, is given as

$$C_A = (A_t - 2\varepsilon_B \cdot \overset{\cdot}{C}_A) / (\varepsilon_A - 2\varepsilon_B)$$

where $\overset{\cdot}{C}_A$ represents the voncentration of $[Fe(Par)_2]^-$ at $t = 0$.

Results

Kinetics of Forward Reaction

The forward reaction is favoured thermodynamically, $\{K_{FeNTA} = 10^{16.26}, K_{FeHEDTA} = 10^{19.86[13]}$ and β_2 of $[Fe(Par)_2]^- = 10^{34.2[14]}\}$. In both systems the forward reaction is first order in each reactant. The observed rate constants for both systems are given in Table 1.

A rate law for both reactions is given as

$$\text{rate} = d[Fe(Par)_2^-] / dt = k[FeL(OH)^-][HR^-] \quad\quad\quad \cdots(2)$$

where $(FeL(OH)^-)$ and (HR^-) are the principal reactive species of iron complexes and Par respectively at the pH of medium. Integration of eqn.(2) yields

$$\log\frac{C_R - 2[FeR_2^-]}{C_{Fe} - [FeR_2^-]} = \frac{C_R - 2C_{Fe}}{2.303} kt + \log\frac{C_R}{C_{Fe}} \quad\quad\quad \cdots(3)$$

A plot of $\text{Log}\dfrac{C_R - 2[FeR_2^-]}{C_{Fe} - [FeR_2^-]}$ vs. t gave a straight line according to equation (3). The second order rate constants k were calculated from the slopes of these straight lines.

Kinetics of Reverse Reaction

The reverse of reactions (1) are thermodynamically not favoured and it becomes possible to force the reverse reactions only by adding a relatively large excess of NTA or HEDTA compared to $[Fe(Par)_2]^-$. The disappearance of $[Fe(Par)_2]^-$ was used to follow the reverse rate.

It has been found that the reverse rate exhibits an inverse first order dependence in Par concentration and a first order dependence each in $[Fe(Par)_2]^-$ and the respective ligands. A rate expression formulated on the basis of above finding is

$$-\frac{d[Fe(Par)_2^-]}{dt} = \frac{k_r[Fe(Par)_2^-][L^{3-}]}{[R^{2-}]} \quad\quad\quad \cdots(4)$$

The integrated form of eqn. (4) is written as

Table 1 Rate Constants for the Reactions of Fe(NTA) and Fe(HEDTA) with Par

temperature $= 25 \pm 0.1$℃, $I = 0.1$ mol $\cdot$ l^{-1} (NaClO$_4$), pH $= 9.0 \pm 0.02$ for NTA reaction

temperature $= 30 \pm 0.1$℃, $I = 0.1$ mol $\cdot$ l^{-1} (NaClO$_4$), pH $= 9.0 \pm 0.02$ for HEDTA reaction

Fe(NTA)-Par Reaction

[Fe(NTA)], (mol $\cdot$ l^{-1})	[Par], (mol $\cdot$ l^{-1})	$k \times 10^{-1}$, (l $\cdot$ mol^{-1} $\cdot$ s^{-1})
5.0×10^{-6}	1.21×10^{-5}	9.82
5.0×10^{-6}	1.81×10^{-5}	9.24
5.0×10^{-6}	2.54×10^{-5}	9.64
5.0×10^{-6}	3.13×10^{-5}	9.91
5.0×10^{-6}	4.17×10^{-5}	11.7
2.88×10^{-5}	1.2×10^{-5}	9.16
3.6×10^{-5}	1.2×10^{-5}	10.14
6.0×10^{-5}	1.2×10^{-5}	10.72
		k(av) $= (10.04 \pm 0.8) \times 10^{1}$, (l $\cdot$ mol^{-1} $\cdot$ s^{-1})

FeHEDTA-Par Reaction

[Fe(HEDTA)], (mol $\cdot$ l^{-1})	[Par], (mol $\cdot$ l^{-1})	$k \times 10^{-1}$, (l $\cdot$ mol^{-1} $\cdot$ s^{-1})
1.0×10^{-5}	2.43×10^{-5}	2.86
1.0×10^{-5}	4.14×10^{-5}	2.6
1.0×10^{-5}	6.87×10^{-5}	2.58
1.0×10^{-5}	8.24×10^{-5}	2.61
1.0×10^{-5}	1.0×10^{-4}	2.54
5.76×10^{-5}	2.4×10^{-5}	2.93
8.4×10^{-5}	2.4×10^{-5}	2.73
1.2×10^{-4}	2.4×10^{-5}	2.77
1.92×10^{-4}	2.4×10^{-5}	2.64
		k(av) $= (2.7 \pm 0.13) \times 10^{-1}$, (l $\cdot$ mol^{-1} $\cdot$ s^{-1})

$$(A_o - A_t') + A_o \ln \frac{A_t'}{A_o} = -\frac{\varepsilon \cdot 1}{2} \cdot k_{obsd}' \cdot t \quad \cdots (5)$$

where A_o is the initial absorbance due to [Fe(Par)$_2$]$^-$, A_t' is the corrected absorbance for [Fe(P$_{ar}$)$_2$]$^-$ at time t, and ε is the molar extinction coefficient of [Fe(Par)$_2$]$^-$ at 496 nm. A plot of left   hand side of equation (5) versus time gives a straight line . The rate constants k_{obsd}' and hence k_r were calculated from the slope of these plots and are given in Table 2. Values of log k_{obsd}' are   plotted against log[L^{3-}]$_T$ in Fig.1. The   slope   of   above plot is found to be one at   higher   ligand   concentration   and   tends   to   zero

at low ligand concentration. This zero order dependence in L^{3-} indicated a slow dissociation of the $[FeR_2]^-$ complex to $[FeR]^+$ and Par. This is followed by further reaction of $[FeR]^+$ with L^{3-} to give $[FeL(OH)]^-$ and $HPar^-$ (vide supra).

Table 2　Kinetics of Decomposition of $[Fe(Par)_2]^-$ by L^{3-} for NTA Reaction

$[Fe^{3+}] = (1.5-2.0) \times 10^{-5} mol \cdot l^{-1}$, $[Par] = (3.0-4.0) \times 10^{-5} mol \cdot l^{-1}$,

temp. $= 25 \pm 0.1℃$, $I = 0.1 mol \cdot l^{-1}$ (NaClO$_4$), pH $= 9.0 \pm 0.02$

for FeHEDTA reaction $[Fe^{3+}] = (0.5-1.0) \times 10^{-5} mol \cdot l^{-1}$,

$[Par] = (1.0-2.0) \times 10^{-5} mol \cdot l^{-1}$　temp. $= 30 \pm 0.1℃$, $I = 0.1 mol \cdot l^{-1}$ (NaClO$_4$),

pH $= 9.0 \pm 0.02$

Fe(Par)$_2$–NTA reaction

NTA(mol $\cdot l^{-1}$)	$k^1_{obsd} \times 10^9$ (mol $\cdot l^{-1} \cdot s^{-1}$)	$k_r \times 10^6$ (s^{-1})
2.0×10^{-2}	25.5	1.28
1.0×10^{-2}	15.9	1.59
8.0×10^{-3}	9.1	1.14
6.0×10^{-3}	8.0	1.33
5.0×10^{-3}	5.4	1.08
2.5×10^{-3}	4.7 *	k_r(av.) $= (1.28 \pm 0.18) \times 10^{-6} s^{-1}$
2.19×10^{-3}	3.9 *	
1.25×10^{-3}	3.7 *	
1.0×10^{-3}	3.8 *	

Fe(Par)$_2$–HEDTA　　reaction

HEDTA(mol $\cdot l^{-1}$)	$k^1_{obsd} \times 10^9$ (mol $\cdot l^{-1} \cdot s^{-1}$)	$k_r \times 10^5$ (s^{-1})
1.92×10^{-3}	24.2	1.26
9.98×10^{-4}	10.0	1.00
7.47×10^{-4}	7.8	1.04
4.97×10^{-4}	5.4	1.08
2.88×10^{-4}	3.2	1.10
1.96×10^{-4}	2.0	1.01
1.25×10^{-4}	1.3 *	k_r(av.) $= 1.17 \pm 0.17 \times 10^{-5} s^{-1}$
8.0×10^{-5}	1.2 *	
6.0×10^{-5}	1.2 *	

* zero order dependence in L^{3-}

pH Dependence of the Forward Rate:

The pH profiles (pH $= -\log [H^+]$ for dilute solutions) for both reactions over the range of

interests are shown in Fig.2. In the case of [Fe(NTA)], the rate was found to increase in the pH range 6−8.5 and then level off. In the case of [Fe(HEDTA)], however, the rate was found to increase with increase of pH above 8.75. There is no levelling off at higher pH, but at lower pH a levelling off occurs (Fig.2). These pH profiles can be explained on the basis of reactivities of different species of [Fe(HEDTA)], [Fe(NTA)], (Fig.3,4) and Par by a procedure outlined in the discussion (vide supra).

Temperature Dependence of Forward and Reverse Rate:

Activation parameters for the forward and the reverse reactions were obtained from the Arrhenius plots drawn in the temperature range 25−45℃ and are given in Table 3.

<div align="center">

Table 3　Activation Parameters

</div>

forward reaction	
(a)　Fe(NTA)+2 Par reaction	(b)　Fe(HEDTA)+2 Par reaction
pH = 9.0 ± 0.02	pH = 10.0 ± 0.02
$\Delta H^{\circ \neq} = 62.6 \pm 0.7$ kJ·mol^{-1}	$\Delta H^{\circ \neq} = 86.1 \pm 2.1$ kJ·mol^{-1}
$\Delta S^{\circ \neq} = 2.9 \pm 1$ J·K^{-1}·mol^{-1}	$\Delta S^{\circ \neq} = 46 \pm 7$ J·K^{-1}·mol^{-1}
reverse reaction	
zero order dependence	
(c)　Fe(Par)$_2$+NTA reaction	
pH = 9.0 ± 0.02	first order dependence
$\Delta H^{\circ \neq} = 41.8 \pm 0.4$ kJ·mol^{-1}	
$\Delta S^{\circ \neq} = -254 \pm 4$ J·K^{-1}·mol^{-1}	$\Delta H^{\circ \neq} = 34.5 \pm 0.4$ kJ·mol^{-1}
(d)　Fe(Par)$_2$+HEDTA reaction	$\Delta S^{\circ \neq} = -237 \pm 13$ J·K^{-1}·mol^{-1}
pH = 10.0 ± 0.02	$\Delta H^{\circ \neq} = 53.2 \pm 21$ kJ·mol^{-1}
$\Delta H^{\circ \neq} = 72.3 \pm 2.0$ kJ·mol^{-1}	$\Delta S^{\circ \neq} = -160 \pm 7$ J·K^{-1}·mol^{-1}
$\Delta S^{\circ \neq} = -171 \pm 6$ J·K^{-1}·mol^{-1}	

Discussion

The results of studies on the forward and reverse reactions of [Fe(] and Par suggest a mechanism given in equations (6)−(8). In the forward reaction the proton generated in step (8) will be consumed by the basic medium.
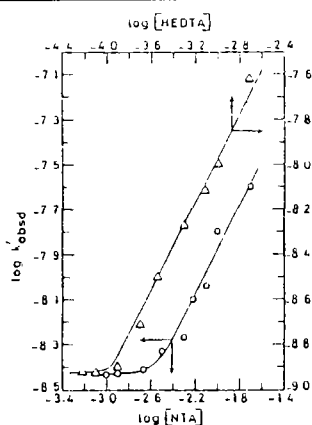
$$[\text{FeL(OH)}]^{-} + \text{HR}^{-} \underset{k_{-1}}{\overset{k_{1}}{\rightleftharpoons}} [\text{RFeL}]^{2-} + \text{H}_2\text{O} \qquad\qquad \text{fast} \cdots (6)$$

Fig.1　Ligand dependence of the observed reverse

rate constants for the reactions of

$[Fe(Par)_2]^-$ with NTA(　) and HEDTA($\triangle$).

The reaction conditions are given in Table 2

Fig.2　Effect of pH on the reactions of $[Fe(NTA)]$ (　) and

$[Fe(HEDTA)]$ ($\triangle$) with Par

$[Fe(NTA)]$ $= (0.5-3.6) \times 10^{-5} mol \cdot l^{-1}$

$[Par]$ $= (2.54-1.2) \times 10^{-5} mol \cdot l^{-1}$

$[Fe(HEDTA)]$ $= 1.0 \times 10^{-5} mol \cdot l^{-1}$

$[Par]$ $= 2.4 \times 10^{-5} mol \cdot l^{-1}$, $I = 0.1 mol \cdot l^{-1}(NaClO_4)$,

temp. $= 25 \degree \pm 0.1 ℃$
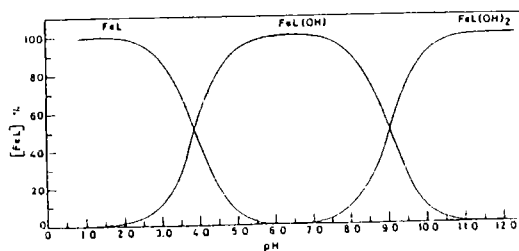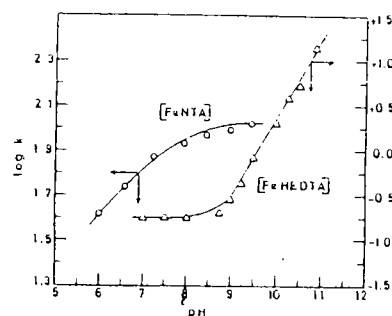
Fig.3　Species distribution of FeHEDTA system as

a function of pH

$[Fe(HEDTA)]$ $= 2.5 \times 10^{-4} mol \cdot l^{-1}$, temp. $= 25℃$
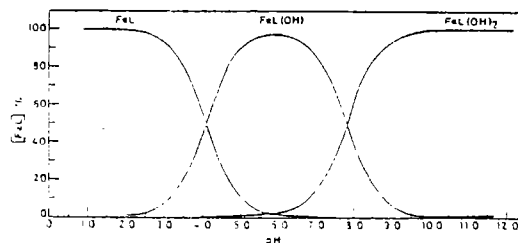
Fig.4　Species distribution of Fe(NTA) system as

a function of pH

$[Fe(NTA)]$ $= 2.5 \times 10^{-4} mol \cdot l^{-1}$, temp. $= 25℃$
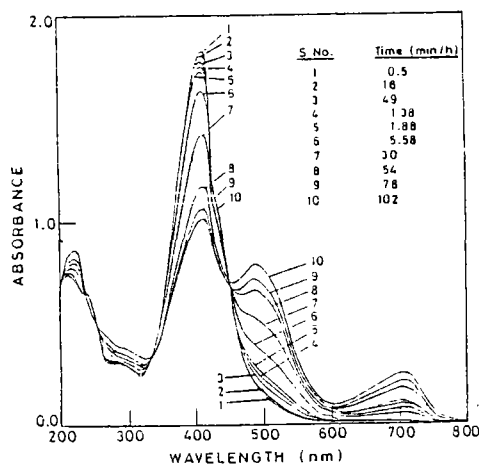
Fig.5

Spectral scan of the reaction mixture of [Fe(HEDTA)] and Par

$[Fe(HEDTA)] = 5.0 \times 10^{-6} mol \cdot l^{-1}$, $[Par] = 5.0 \times 10^{-5} mol \cdot l^{-1}$,

pH $= 9.0 \pm 0.02$, $I = 0.1 mol \cdot l^{-1}(NaClO_4)$, temp. $= 25 \degree \pm 0.1 ℃$.

time (min / h):0.5(1),16(2),49(3),1.38(4),1.88(5),5.58(6),

30(7),54(8),78(9),102(10)

$$[RFeL]^{2-} \underset{k_{-2}}{\overset{k_2}{\rightleftharpoons}} [FeR]^+ + L^{3-} \qquad \text{r.d.s.} \cdots(7)$$

$$[FeR]^+ + HR^- \underset{k_{-3}}{\overset{k_3}{\rightleftharpoons}} [FeR_2]^- + H^+ \qquad \text{fast} \cdots(8)$$

Spectral scan of the reaction mixture (Fig.5) shows that $[RFeL]^{2-}$ is not present in appreciable amounts. Therefore, a steady state approximation can be applied to $[RFeL]^{2-}$. The rate equation for the formation of $[FeR_2]^-$ is then given by

$$\frac{d[FeR_2^-]}{dt} = \frac{k_1 k_2}{k_{-1} + k_2} [FeL(OH)^-][HR^-] \qquad \cdots(9)$$
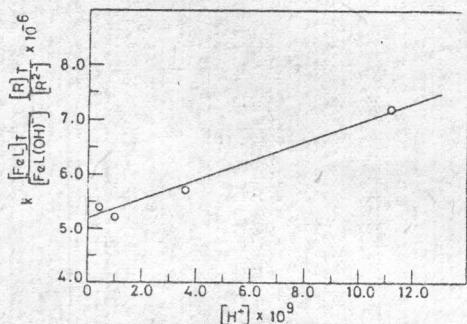
Fig.6

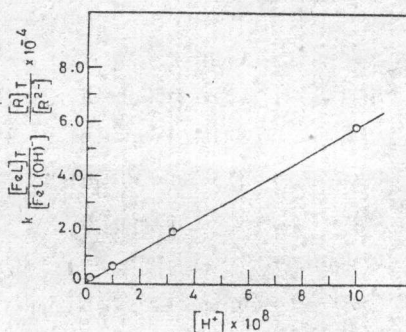Resolution of rate constants for the reactions of $[Fe(NTA)OH]^-$ and $[Fe(NTA)(OH)_2]^{2-}$ with HR^-

Fig.7

Resolution of rate constant due to the reaction of $[Fe(HEDTA)OH]^-$ and HR^-

This is consistent with the experimental observation that the forward reaction is first order in each reactant and overall second order (Eqn.2).

The reverse reaction between $[FeR_2]^-$ and L^{3-} is zero order in (L^{3-}) at low ligand concentration. This shows a dissociation of the bis complex to the monocomplex $[FeR]^+$ and HR^- according to eqn. (8). The rate law for the reverse reaction is given by

$$\text{Rate} = k_{-2}[FeR][L^{3-}] = \frac{k_{-2} K_3^{-1}}{K_{HR}} \cdot \frac{[FeR_2^-][L^{3-}]}{[R^{2-}]} \qquad \cdots(10)$$

This is also consistent with the experimental observation that the reverse reaction is first order in each $[FeR_2]^-$ and L^{3-} and inverse first order in R^{2-} (Eqn.4). In this expression K_{HR} is the protonation constant of Par.

The pH dependence of the observed rates can be used for evaluating the rate constants due to reactant species present at different pH. The relative concentration of various species calculated by a computer program due to Perrin and Sayce[15] is given in Fig.4. In the pH range 6—10 the complex $[Fe(NTA)]$ exists as $[FeL(OH)]^-$ and $[FeL(OH)_2]^{2-}$ while the Par as HR^- only. The observed rate can be resolved by an algebric procedure outlined below:

$$\text{Rate} = k[FeL]_T[R]_T = \{k_{HR}^{FeL(OH)}[FeL(OH)^-] + k_{HR}^{FeL(OH)_2}[FeL(OH)_2^{2-}]\}[HR^-] \qquad \cdots(11)$$

The subscript T in the above expression indicates the total concentration of both species in all their forms. Algebric manipulation yields an expression suitable for graphical treatment given below.

$$k \cdot \frac{[FeL]_T}{[FeL(OH)^-]} \cdot \frac{[R]_T}{[R^{2-}]} = k\{1 + K_1 K_w / [H^+]\}\{1 + K_{HR}[H^+]\}$$

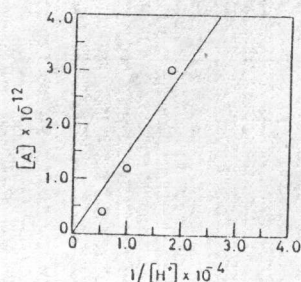$$= \{k_{HR}^{FeL(OH)} K_{HR}[H^+] + k_{HR}^{FeL(OH)2} K_{FeL(OH)_2} \cdot K_{HR} \cdot K_w\} \qquad \cdots(12)$$

Fig.8

Resolution of rate constant due to the reaction of
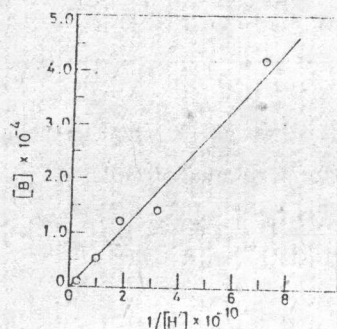
$[Fe(HEDTA)(OH)_2]^{2-}$ and HR^-

Fig.9

Resolution of rate constant for the

reaction of $[Fe(HEDTA)(OH)_2]^{2-}$ and R^{2-}

$$\text{where}[FeL]_T = [FeL(OH)^-] + [FeL(OH)_2^{2-}] = [FeL(OH)^-](1 + K_1 K_w / [H^+])$$

$$\frac{[FeL]_T}{[FeL(OH)^-]} = \frac{1 + K_1 K_w}{[H^+]}$$

In the above expressions

$$K_1 = \frac{[FeL(OH)_2^{2-}]}{[FeL(OH)^-][OH^-]} = 10^{6.2 \, [16]}$$

K_w is ionization constant of water at 25℃ and K_{HR} is the protonation constant of Par $(= 10^{12.5})$

A plot of left hand side of eqn. (12) versus $[H^+]$ gives a straight line (Fig.6) and the rate constants due to $[FeL(OH)]^-$ and $[FeL(OH)_2]^{2-}$ are calculated from the slope and intercept respectively (Table 4).

In the pH range 7—11, $[Fe(HEDTA)]$ exists as $[FeL(OH)]^-$ and $[FeL(OH)_2]^{2-}$ and Par as HR^- and R^{2-} (Fig.3). As in the case of $[Fe(NTA)]$, the rate can be resolved again by algebric procedure outlined above.

$$\text{Rate} = k[FeL]_T[R]_T \qquad \cdots(13)$$

where FeL represents the $[Fe(HEDTA)]$ complex. The right hand side of above equation can, by making use of protonation constants of Par and stability constant of $[FeL(OH)_2]^{2-}$, be written as

$$k[FeL]_T[R]_T = k_{HR}^{FeL(OH)}[HR^-][FeL(OH)^-] + k_R^{FeL(OH)}[R^{2-}][FeL(OH)^-]$$

$$+ k_{HR}^{FeL(OH)_2}[HR^-][FeL(OH)_2^{2-}] + k_R^{FeL(OH)_2}[R^{2-}][FeL(OH)_2^{2-}] \qquad \cdots(14)$$

Table 4 Resolved Rate Constants for the Reaction of Fe(NTA)
and Fe(HEDTA) with Par

Fe(NTA)—Par reaction	Fe(HEDTA)—Par reaction
$k_{HR}^{FeL(OH)} = 5.6 \times 10^1 \text{ l} \cdot \text{mol}^{-1}\text{s}^{-1}$	$k_{HR}^{FeL(OH)} = 1.8 \times 10^{-1} \text{ l} \cdot \text{mol}^{-1}\text{s}^{-1}$
$k_{HR}^{FeL(OH)_2} = 1.04 \times 10^2 \text{ l} \cdot \text{mol}^{-1}\text{s}^{-1}$	$k_{HR}^{FeL(OH)_2} = 4.97 \times 10^{-1} \text{ l} \cdot \text{mol}^{-1}\text{s}^{-1}$
	$k_{R}^{FeL(OH)_2} = 5.85 \times 10^2 \text{ l} \cdot \text{mol}^{-1}\text{s}^{-1}$

In the pH range 7–8.75, the term containing $[R^{2-}]$ and $[FeL(OH)_2^{2-}]$ can be neglected and equation (14) transforms to equation (15).

$$k\frac{[FeL]_T}{[FeL(OH)^-]} \cdot \frac{[R]_T}{[R^{2-}]} = k_{HR}^{FeL(OH)} \cdot K_{HR}[H^+] \qquad \cdots(15)$$

By plotting left hand side of equation (15) versus $[H^+]$, we get a straight line with an intercept equal to zero and slope $= k_{HR}^{FeL(OH)} \cdot K_{HR}$ (Fig.7) from which $k_{HR}^{FeL(OH)}$ can be evaluated.

In the pH range 8.75–9.25, however, the term containing $[R^{2-}]$ can be neglected and equation (14) transforms to equation (16).

$$K\frac{[FeL]_T}{[FeL(OH)^-]} \cdot \frac{[R]_T}{[R^{2-}]} \cdot \frac{1}{[H^+]} - K_{HR}^{FeL(OH)} \cdot K_{HR}$$
$$= k_{HR}^{FeL(OH)_2} \cdot K_{FeL(OH)_2} \cdot K_{HR} \cdot K_w \cdot \frac{1}{[H^+]} \qquad \cdots(16)$$

For simplification we may set

$$A = \{k\frac{[FeL]_T}{[FeL(OH)^-]} \cdot \frac{[R]_T}{[R^{2-}]} \cdot \frac{1}{[H^+]} - k_{HR}^{FeL(OH)} \cdot k_{HR}\} \qquad \cdots(17)$$

A plot of A versus $1 / [H^+]$ yields a straight line passing through the origin (Fig.8) with a slope equal to $k_{HR}^{FeL(OH)_2} \cdot K_{FeL(OH)_2} \cdot K_{HR} \cdot K_w$ from which $k_{HR}^{FeL(OH)_2}$ can be obtained.

Above pH 9.5, on the other hand, the term containing $[FeL(OH)^-]$ can be neglected, and equation (14) transforms to equation (18).

$$k\frac{[FeL]_T}{[FeL(OH)^-]} \cdot \frac{[R]_T}{[R^{2-}]} - k_{HR}^{FeL(OH)_2} \cdot K_{HR} \cdot K_{FeL(OH)_2} \cdot K_w$$
$$= k_{R}^{FeL(OH)_2} \cdot K_{FeL(OH)_2} \cdot K_w \cdot \frac{1}{[H^+]} \qquad \cdots(18)$$

For simplification we may set

$$B = \{K\frac{[FeL]_T}{[FeL(OH)^-]} \cdot \frac{[R]_T}{[R^{2-}]} - K_{HR}^{FeL(OH)_2} \cdot K_{HR} \cdot K_{FeL(OH)_2} \cdot K_w\}$$

A plot of left hand side of equation (18) versus $1 / [H^+]$, again yields a straight line (Fig.9) passing through the origin with a slope equal to $k_R^{FeL(OH)_2} \cdot K_{FeL(OH)_2} \cdot K_W$ which enables us to obtain $k_R^{FeL(OH)_2}$. It is not possible to calculate the fourth rate constant $K_R^{FeL(OH)}$, because the species $[FeL(OH)^-]$ exists only upto pH 10 and $[R^{2-}]$ exists above pH 10.5. The concentration of any one in the presence of other is negligibly small and the rate, therefore, very slow. All the resolved rate constants are listed in Table 4.

In the forward reaction the mixed ligand intermediate $[RFeL]^{2-}$ gives $[FeR]^+$ and $[L]^{3-}$ (Equation 7). It is presumed that Par is not as flexible as aliphatic polyamines. It is unlikely that NTA or HEDTA would react with Par complexes via a stepwise removal of the donor atoms of Par from the coordination sphere of the central metal as postulated previously in the substitution of polyamine complexes of nickel by EDTA [2], DTPA [17] and PDTA [18]. TMDTA [19] and HEDTA [20]. As soon as one donor atom of Par is removed from the central metal ion of the intermediate [RF̈eL], the other two also get detached. This step should, therefore, be the rate-determining one.

The moderately high activation enthalpies and positive entropies of activation (Table 3) for the forward reactions are also in accord with the proposed rate-determining step where a bond dissociation is taking place. Thus, the mechanism is dissociative rather than an associative one. A comparison of activation parameters of the reverse reactions in conditions of first and zero order dependences in [Ligand] shows that the ligand dependent pathway is associated with lower activation enthalpy than the ligand independent path. The entropies of activation for the reverse reaction (when order is one in ligand) is large and negative as expected for the reverse reaction of the second and rate determining step (eqn. 7). However, the entropies of activation for the dissociation of Fe(Par)$_2$ complex (eqn. 8, when order is zero in ligand) is not easily rationalized. It would be necessary to give a detailed consideration to the solvation of the reactant and the transition state species in the dissociation step and this is not easily done. We are, therefore, content with reporting the experimental values without comment.

A repetitive scan (Fig. 5) of the forward reaction for Fe(HEDTA)–Par system shows the formation and decay of the product and the reactant species respectively. The growth of peaks at 720 and 496 nm is due to formation of $[Fe(Par)_2]^-$. There is also a continuous decrease of absorbance at 414nm due to consumption of Par during the course of reaction. The shift of peak at 210 nm to 225 nm also shows the formation of $[Fe(Par)_2]^-$ and release of HEDTA. The appearance of isosbestic points at 450 and 335nm suggests that $[Fe(Par)_2]^-$ and Par coexist during the course of reaction. The spectral changes occuring during a kinetic run of the reverse reaction (not shown) also support these conclusions.

To summarise, the substitution of [FeL] complexes by Par takes place in three steps (eqns. 6–8) through the formation of a mixed ligand complex intermediate [RFeL]. The dissociation of this intermediate to $[FeR]^+$ and L^{3-} constitutes the rate determining step. Intermediate [RFeL]. The dissociation of this intermediate to $[FeR]^+$ and L^{3-} constitutes the rate determining step. The addition of second molecules of Par is fast resulting in the formation of $[FeR_2]^-$ finally.

References

〔1〕 Rogers, D.W., Aikens, D.A., and Reilley, C.N., *J.Phys. Chem.*,**66**,1582 (1962).

〔2〕 Rorabacher D.B., and Margerum, D.W., *Inorg . Chem.*, **3**, 382(1964).

〔3〕 Baddley W.H., and Basolo, F., *J.Amer. Chem. Soc.*,**88**,2944 (1966).

〔4〕 Tanaka,M., Funahashi, S., and Shirai, K., *Inorg. Chem.*, **7**, 573 (1968).

〔5〕 Rabenstein D.L., and Kula, R.J.,*J. Amer. Chem. Soc.*,**91**,2492 (1969).

〔6〕 Funahashi, S.,Yamada,S. and Tanaka, M.,*Bull. of Chem. Soc. of Japan*, **43**, 769 (1970).

〔7〕 Funahashi S. and Tanaka, M.,*Inorg.Chem.*, **8**, 2159 (1969).

〔8〕 Desai, A.G.,Dodgen H.W. and Hunt, J.P.,*J.Amer. Chem. Soc.*,**92**, 798 (1970) and refs. therein.

〔9〕 Funahashi S.,and Tanaka, M.,*Inorg. Chem.*,**9**, 2092 (1970).

〔10〕 Funahashi, S.,Tabata M.,and Tanaka, M.,*Bull. of Chem. Soc.Japan*, **44**, 1586 (1971).

〔11〕 Funahashi, S.,Yamada S.,and Tanaka, M.,*Inorg. Chem.*, **10**, 257 (1971).

〔12〕 Schwarzenbach, G.,Complexometric Titrations (Int. Sci. Pub., N.Y.,P.77,(1985).

〔13〕 Martell A.E.,Stability Constants of Metal Ion Complexes,(Alden Press, Oxford), No.25,(1985).

〔14〕 Hoshino, H.,and Yotsuyanagi, T.,*Talanta*, **31**, 525 (1984).

〔15〕 Perrin, D.D.,and Sayce, I.G.,*Talanta*, **14**, 833 (1967).

〔16〕 Martell,A.E.,Critical Stability Constants, Plenum press,(New York and London),Vol.1,(1974).

〔17〕 Bajaj,H.C., and Nigam, P.C.,*Ind.J.Chem.*, **23A**, 8(1984).

〔18〕 Naik, R.M.,and Nigam, P.C.,*Ind.J.Chem.*, **26A**, 205 (1987).

〔19〕 Kumar,K., and Nigam, P.C.,*Inorg.Chem.*, **20**, 1623 (1981).

〔20〕 Bajaj, H.C.,Kumar K.,and Nigam, P.C.,*Ind.J.Chem.*, **19A**, 1070 (1981).